Subseasonal prediction for bloom dates of tart cherries in Utah and Michigan, USA: Merging phenological models with CFSv2 forecast

Parichart Promchote[1,3]*, S.-Y. Simon Wang[1,2], Brent Black[1], and Paul G. Johnson[1]

[1]*Department of Plants, Soils, and Climate, Utah State University, Logan, UT, USA*

[2]*Utah Climate Center, Utah State University, Logan, UT, USA*

[3]*Department of Agronomy, Kasetsart University, Bangkok, Thailand*

**Corresponding author address*: Parichart Promchote, Department of Agronomy, Kasetsart University, 50 Phaholyothin Road, Jatujak, Bangkok, 10900, Thailand.

Email: parichart.pr@ku.th

Abstract

Temperate fruit trees require chilling for rest completion, followed by sufficient heat accumulation for onset of growth and bloom. The application of phenological models to predict bloom dates has been widely used in orchard management. Examples of such application include selecting adapted cultivars less prone to early bloom, predicting needs for frost protection, and preventing damage from late spring freezes. This study merged the *Utah* (chill) and ASYMCUR (forcing) phenological models by combining chill units and heat units (measured in growing degree hours) to predict bloom dates of tart cherries (*Prunus cerasus* L.) in Utah and Michigan, the top producing states of the USA. It was found that the modified *Utah* model improves the estimation of chill units compared to the original one, while the original *Utah* model may still be suitable for use in the colder winter of Michigan (with its later bloom dates than Utah). The combined models were applied with the temperature predicted by the Climate Forecast System v2 (CFSv2) model. The prediction was applied twice a month, starting from 1 February to 1 May. The *Utah*-ASYMCUR model using the forecasted temperature from CFSv2 exhibits subseasonal performance in predicting the bloom dates for 6 weeks in advance. The prediction can offer growers a way to mitigate extreme climate anomalies.

Keywords: chill models, heat models, bloom dates, tart cherries, CFSv2, subseasonal prediction

1. Introduction

Temperate fruit crops are most susceptible to cold temperature damage during the period near full bloom. For tart cherry (*Prunus cerasus* L.) near bloom, the critical temperatures at which 10% and 90% of fruiting buds are killed are -2.2°C and -4.4°C respectively (Longstroth 2007). In 2012, the Michigan tart cherry industry, typically the largest in the United States, experienced catastrophic crop losses (USDA 2017; Fig. 1a) due to a combination of an anomalously warm spring that brought on early bloom followed by consecutive days of freezing temperatures during bloom (Ault et al. 2013; Rill 2016). In Utah, the second largest tart cherry producing state, damage from freeze events near bloom is also common, as was the case in May 2002 (Fig. 1b; NASS 2002). Much of the commercial fruit production in Utah is situated in high elevation mountain valleys (1,400 to 1,525 m elevation) with a semi-arid climate, with wide temperature fluctuations in late winter and early spring. These temperature fluctuations can result in crop failure when they occur during bloom.

Understanding the frequency of and predicting crop losses due to spring frost is an important step in sustaining the fruit industry under the warming climate. Observational analysis shows that the onset of spring across western North America has advanced at a rate ranging from 1.5 to 3 days per decade (Schwartz et al. 2006, 2013), accompanied by a large yearly fluctuation up to 30 days (Ault et al. 2013). Springtime warming is accompanied by a pronounced declining trend in the snowpack and earlier snowmelt in the western US (Cayan et al. 2001; Dettinger et al. 2004; Hamlet et al. 2005; McCabe and Wolock 2007) including Utah (Gillies et al. 2012). These phenomena have accelerated bloom of many tree species (i.e., Ault et al. 2013; Ellwood et al. 2013) while increasing the risk of spring freeze damage (Augspurger 2013). Subsequently, developing an extended forecast for spring climate and full bloom date of crops is a necessary next step to help mitigate risk of damage in the fruit industry. To the authors' knowledge, there is no subseasonal prediction (2 weeks to 2 months lead time) of bloom dates for tart cherries in Utah and Michigan.

The objective of this study is to test the feasibility of subseasonal prediction by combining common phenological models for tart cherries with climate model forecasts. We combined two different models, i.e. the *Utah*-chill model and the ASYMCUR-forcing model, which were developed based on peach and cherry trees in Utah and Michigan (Richardson et al. 1974; Anderson et al. 1986). These models have been widely tested for a variety of fruit and forest trees (Cesaraccio et al. 2004; Melo-Abreu et al. 2004; Pérez et al. 2008; Luedeling and Brown 2011; Miranda et al. 2013; Maulión et al. 2014). In our analysis, we evaluate the prediction of bloom dates using a subseasonal climate prediction model. Phenological and meteorological datasets were obtained from sites in Michigan and Utah, representing each state's most important tart cherry growing region. The details of these models and the data used are introduced in section 2. Section 3 provides the results and discussion in the two parts: section 3.1 presents the modeling and validation analysis results, and section 3.2 presents the subseasonal forecast results. Discussion and conclusion are given in section 4 and 5, respectively.

2. Materials and methods

2.1 Bloom date and meteorological data

Dates of full bloom (BBCH65) of 'Montmorency' tart cherries were collected from a commercial orchard near West Payson, Utah, and from Michigan State University's Northwest MI Horticultural Research Center, Traverse City, Michigan (location in Fig. 1c). The datasets cover the periods of 1983-2014 for Traverse City, Michigan (TC-MI) and 1986-2016 for West Payson, Utah (WP-UT). Temperature data were obtained from automated weather stations located within the orchards (WP-UT, 40.135°N, -111.820°W, 1404.5 m a.s.l.; and TC-MI 44.8831°N, -85.6777°W, 247 m a.s.l.) and data stored and managed by the Utah Climate Center (https://climate.usu.edu) for Utah and by the Enviro-weather Automated Weather Station Network (https://mawn.geo.msu.edu) for Michigan, respectively. The Utah data set contains hourly records for 2010-2017, with 7.1% of missing values, and daily data for 2004-2017, with 0.25% (0.29%) of missing Tmax (Tmin). The Michigan data set includes both hourly and daily data for 2000-2017, with missing values for hourly, daily-Tmax and daily-Tmin data at rates of 0.12%, 0.19% and 0.66%, respectively. Missing values of temperature were estimated by using linear interpolation.

Since phenological models (chill and heat models) require hourly data as inputs, daily minimum temperature (Tmin) and maximum temperature (Tmax) during 2004-2017 for WP-UT and 2000-2017 for TC-MC were converted to hourly temperature by using two methods, the triangular approximation (Cortázar-Atauri et al. 2009) and Linvill's method (Linvill 1990), as follows:

- *Triangular approximation*: The method consists of linear interpolation between Tmax/Tmin of day *n* [Tmax(*n*) / Tmin(*n*)] and Tmin of day *n+1* [Tmin(*n+1*)]. It assumes a daylength of 12 hours and calculates hourly temperature of each day *n* at time *h* [T(*h,n*)] based on Eq.1 and Eq.2:

$$\text{if } h \leq 12 \quad \text{then} \quad T(h,n) = Tmin(n) + h\,[(Tmax(n) - Tmin(n))/12] \qquad (1)$$

$$\text{if } h > 12 \quad \text{then} \quad T(h,n) = Tmax(n) - (h-12)\,[(Tmax(n) - Tmin(n+1))/12] \qquad (2)$$

- *Linvill's method*: The model development is based on daytime solar cycle and nighttime cooling curve. Hourly temperature from sunrise to sunset was estimated using Eq.3; where T(t) is temperature at time t after sunrise and DL is daylength (in hours). The nighttime hourly temperature was estimated by using Eq.4; where T(t) is temperature at time $t > 1$ hour after sunset and Ts is the sunset temperature obtained from Eq.3. The first method requires only temperature data while the second method requires datasets of temperature, sunrise-sunset times and day lengths for the calculation. Sunrise and sunset times are obtained from US Navy website (htpps://aa.usno.navy.mil/ data/docs/RS_OneDay.php). Daylength is the difference between sunrise and sunset times.

$$T(t) = (Tmax - Tmin) \times \sin[(\pi \times t)/(DL + 4)] + Tmin \qquad (3)$$

$$T(t) = Ts - [(Ts - Tmin)/\ln(24 - DL)] \times \ln(t) \qquad (4)$$

We compared these two methods and found Linville's method to perform more realistically, concerning daylength variation in each season and location than the hourly data. Nonetheless, the triangular approximation is a simpler method and was also used.

2.2 Phenological models

Phenological models predict bud development through two phenological phases: endodormancy and ecodormancy. The process of endodormancy release (rest completion) requires chilling temperature for a sufficient period of time and can be predicted by several chill models (i.e. Bennett 1949; Weinberger 1950; Richardson et al. 1974; Fishman et al. 1987a, b; Erez et al. 1990). After rest completion, warm spring temperatures (heat accumulation) release ecodormancy and buds resume growth. The heat accumulation can be estimated by forcing or heat models (i.e. Richardson et al. 1982; Anderson et al. 1986; Bonhomme 2000). Spring heat accumulation alone has been used to predict bloom dates of woody trees (Hänninen 1995; Fu et al. 2012) but the prediction is more precise when both chilling and heat accumulation are included (i.e., Melo-Abreu et al. 2004; Miranda et al. 2013; Maulión et al. 2014; Chuine et al. 2016). Hereafter, combined chill and heat models were used to predict bloom dates.

The methodological steps for estimating and predicting bloom dates in WP-UT and TC-MI are described in Figs. 2a and 2b respectively. We used the *Utah* model to estimate end date of endodormancy based on chill units (CH; Fig. 3; Richardson et al. 1974) and sequentially used the asymmetric curvilinear model (ASYMCUR model) to estimate budburst (Fig. 2 Steps A and B) based on heat units in growing degree hours (GDH) (Richardson et al. 1982; Anderson et al. 1986). ASYMCUR requires hourly temperature (TH), with 4 ºC as base temperature (TB), 25 ºC as optimum temperature (TO) and 36 ºC as the maximum critical temperature (TM), TO-TB represents the amplitude of the growth curve (A), and 1.0 as a stress factor of the fruit tree (F) for the computation. See the following two equations (Fig. 2 steps B and C; see Table 1 for abbreviations):

$$\text{if TH} \leq \text{TO then GDH} = \text{F} \cdot \text{A}/2\,[1 + \text{cosine}\,(\pi + \pi\,(\text{TH-TB})/(\text{TO-TB}))] \quad (5)$$

$$\text{if TH} > \text{TO then GDH} = \text{F} \cdot \text{A}\,[1 + \text{cosine}\,(\pi/2 + \pi/2\,(\text{TH-TO})/(\text{TM-TO}))] \quad (6)$$

The combined *Utah*-ASYMCUR models (hereafter "*Utah*-ASYMCUR") were validated using the phenoclimatography values distributed by Anderson et al. (1986) and updated here with the new datasets of weather and bloom dates for the Montmorency tart cherry. By using the *Utah*-ASYMCUR combined model, date of chilling inception of each year was specified by the maximum negative number of chill unit accumulation. Rest completion date was the date when chill accumulation reached 954 units (Anderson et al. 1986). Thereafter GDH was calculated. Full bloom date was indicated when 6130 GDH (Anderson et al. 1986) were accumulated.

The two models were subsequently modified before being used to predict bloom dates (Fig. 2 Step C) because the original combined model produced a late estimation of bloom dates. This assumes the models under-estimate either chill or heat unit accumulation. For the $Utah_{(\text{modified})}$ model (Fig. 3), temperature scales for chill unit contribution were adjusted based on the temperature curves reported by Anderson et al. (1986), while temperatures below 0 °C would not accumulate chill units. Likewise, temperatures 14 °C and above would reduce chill units. This is similar to modifications previously reported for improved estimates for blueberries and blackberries (Warmund and Krumme 2005; Warmund 2015). Here we tested incremental changes in the TB used in the ASYMCUR model (Eq.3) at 0.5 °C increments from 0 °C to 4 °C. We found that 2 °C TB better predicted heat accumulation during the early phase in the ASYMCUR curve (compared to 4 °C TB).

This finding is similar to the correction for heat unit accumulation during the lag phase in a curvilinear model reported by Black et al. (2008).

Accordingly, we selected the modified combined models (*Utah*$_{\text{(modified)}}$-ASYMCUR) to predict bloom dates for WP-UT, whereas the combined original-*Utah* and modified-ASYMCUR models (*Utah*-ASYMCUR$_{\text{(Tbase-2)}}$) was used for TC-MI (Fig. 2 Step C).

2.4 Model validation

The performance of phenological models to estimate bloom dates was evaluated by comparing the observation values (O) with the modeled estimation (P). The indices are correlation coefficients (*r* or CORR), root mean square error (RMSE), and model efficiency (EF; Eq. 7) (Nash and Sutcliffe, 1970). Here, *r* reflects whether the observations and predicted values are trending in the same direction while RMSE and EF quantify the bias. The EF can be from -∞ to +1 with +1 indicating a perfect fit, 0 indicating the predictions are as accurate as the observed mean (so-called the climatology), while a negative number indicates that the model prediction is lower than using the observed mean as a predictor.

$$EF = 1 - \frac{\sum_{i=1}^{n}(O_i - P_i)^2}{\sum_{i=1}^{n}(O_i - \overline{O_i})^2} \quad (7)$$

2.3 Climate prediction: CFSv2 Model

Climate hindcast data are outputs from the NCEP Climate Forecast System version 2 (CFSv2) (Saha et al. 2014) referring to “past prediction” made with the past observations in order to compare the model forecast with the actual events. These past predictions were generated for different lead times before actual bloom dates, which were then compared with the observed bloom dates; these are outlined in Fig. 2 Steps D and E. Two CFSv2 datasets with a near 1^{o} long. x lat. resolution were used, the CFS Reforecast "High-Priority" subset (CFS-R; 2000-2011) and the CFSv2 Operational Forecasts (CFS-OF; 2011-2017). Data of maximum and minimum surface air temperature (Tmax and Tmin) at 2-meter above ground over the period 2000-2017 were used. We obtained the time series of Tmax and Tmin from the nearest model grid points of the WP-UT weather station (40.157^{o}N, -111.562^{o}W) and the TC-MI weather station (44.882^{o}N, -85.312^{o}W).

The bloom date prediction was applied twice each month with forecasts initiated on 1st and 15th of each month. For CFS-R that was available every 5 days, the initialization date nearest to the start of the month and the nearest date to 15th were used. The CFSv2 model was run in 6-hour intervals (00, 06, 12, 18Z) per day so each daily CFSv2 ensemble contained four members. CFSv2-air temperature has a cold bias from the observed dataset and this cold bias is greater in Tmax than in Tmin (example shown in Fig. S1). Thus, using this dataset, the highest value of Tmax from all ensemble members was selected to represent the daily Tmax. To obtain daily Tmin, we averaged all Tmin values from every ensemble and members. These methods provided low RMSE and mean difference between the CFSv2 and the observed daily Tmax/Tmin.

We evaluated the prediction starting approximately 3 months before the bloom dates (Fig. 2 Step E): 1 February (CFS0201), 15 February (CFS0215), 1 March (CFS0301), 15 March (CFS0315), 1 April (CFS0401), 15 April (CFS0415), and 1 May (CFS0501). The average bloom dates (± standard deviation) were designated as 11 May for TC-MI (± 9 days; standard deviation; 2001-2014) for TC-MI and 28 April for WP-UT (± 9 days; 2005-2016) for WP-UT. The actual bloom dates were designated as day-0 (no lead time). Thus, we forecasted on seven lead times (day-10, day-26, day-40, day-57, day-71, day-85, and day-99) for TC-MI and six lead times (day-13, 27-day, day-44, day-58, day-72, and day-86) for WP-UT. The CFSv2 forecast skills (alternatively "model performance" or "predictability") were validated by comparing to the day-0 prediction (Fig. 2 Step D).

Daily Tmax and Tmin from CFSv2 forecasts were statistically downscaled through common bias correction approaches (Hawkins et al. 2013; Navarro-Racines and Tarapues-Montenero 2015), by adjusting the means and variability in each month to be nearest to the observation. The calculation is described in Eq.8, where T_{CFSadj} is adjusted-CFSv2 temperature, $\overline{T_{ob}}$ is the mean of observed temperature (T_{ob}), $\overline{T_{CFS}}$ is mean of original-CFSv2 temperature (T_{CFS}), $RMSE_{ob}$ and $RMSE_{CFS}$ are root mean square errors of T_{ob} and T_{CFS}. The period to calculate mean and RMSE are 2004-2017 and 2001-2017 for WP and TC, respectively. The RMSE is calculated by using Eq.9; where O_i are observed values and P_i are predicted values derived based on linear regression model.

$$T_{CFSadj} = \overline{T_{ob}} + \frac{RMSE_{ob}}{RMSE_{CFS}} \times (T_{CFS} - \overline{T_{CFS}}) \tag{8}$$

$$RMSE = \sqrt{\frac{\sum_{i=1}^{n}(O_i - P_i)^2}{n}} \tag{9}$$

3. Results

3.1 Modeled bloom dates

3.1.1 Original models

Performance of the *Utah*-ASYMCUR model in estimating bloom dates of tart cherries is displayed in Fig. 4a for TC-MI and Fig. 5a for WP-UT. Panels a1 show the comparison among observed dates and estimated dates from observed-hourly temperature (T), estimated-hourly T from daily T by using Linvill's method (daily-Linvill) and Triangular approximation (daily-Triangular). Bias of the estimation from hourly, daily-Linvill and daily-Triangular data is given in panels a2, a3 and a4, respectively. Bars depict the difference in days between the estimated and observed dates, where positive bars indicate a late bias and negative bars indicate an early bias. Model biases are also expressed by correlation coefficients (*r*), efficiency (EF), and root mean square error (RMSE) that are given in brackets at the top of each panel. Figs. 4a1 and 5a1 illustrate interannual variability of the observed bloom dates and show no clear trends during the study periods for either location.

As shown in Figs. 4a2–a4, the estimated bloom dates for TC-MI agree across the three datasets and are highly correlated with the observations (r = 0.95). Nonetheless, the models estimated bloom dates are 8.79, 6.17 and 7.46 days behind with the use of hourly, daily-Linvill and daily-Triangular datasets, respectively, accompanying large biases with low EF scores of 0.05, 0.53, and 0.31. Both models estimated the bloom dates well for WP-UT based on their high correlations with the observations (r = 0.93 to 0.94) (Figs. 5a2-a4). The biases of using hourly, daily-Linvill and daily-Triangular datasets are 8.28, 4.74, and 5.97 days, respectively, with the EF scores of 0.09, 0.70, and 0.52. The lower EF and higher RMSE (i.e. larger bias) when using hourly temperature compared to the daily model reflect the effect of missing hourly observations, particularly in 2011 (7.1%). The significant correlation coefficients suggest that *Utah*-ASYMCUR can predict the interannual variation of bloom dates, albeit with a relatively high bias.

3.1.2 Modified models

Figure 4b displays the performance of *Utah*-ASYMCUR$_{(Tbase\text{-}2)}$, which modified ASYMCUR using a base temperature of 2^{o}C, to estimate bloom dates of tart cherries for TC-MI. The time series of estimated dates from all three datasets fit well with the observed dates (Fig. 4b1). It is noteworthy that the *Utah*-ASYMCUR$_{(Tbase\text{-}2)}$ significantly improved the model efficiency (0.89 to 0.93) and correlation coefficients (0.98 to 0.99) (Figs. 4b2-b4). The estimation is early, yet the bias from using hourly, daily-Linvill and daily-Triangular data are reduced to 2.31, 2.95, and 2.78 days, respectively.

The estimated bloom dates for WP-UT are noticeably improved in the *Utah*$_{(modified)}$-ASYMCUR model (Fig. 5b). The time series of observed and estimated dates from the hourly, daily-Linvill and daily-Triangular consistently trend together (Fig. 5b1). The EF scores (0.63, 0.57) and RMSE (5.24, 5.71) are similarly improved for the hourly and daily-Triangular data, compared to those from the original model (Figs. 5b2, 5b4). Note that the difference between estimated and observed dates remain high in some years (i.e., 2005, 2010, 2011, 2012) according to their high RMSE (4.82-5.71 days) and low EF scores (0.57-0.69) (Figs. 5b2-b4).

Comparison of the modified models (Figs. 4b, 5b) suggests that the daily-Linvill outperforms the daily-Triangular. Additionally, either the daily-Linvill or daily-Triangular datasets can substitute for the hourly record, leading support to the widely used daily temperature substitution in fruit-tree phenological models.

3.2 Climate prediction of bloom dates

3.2.1 Predictability of unadjusted-CFSv2 data

To predict bloom dates, we ran the *Utah*$_{(\mathrm{modified})}$-ASYMCUR model for WP-UT and *Utah*-ASYMCUR$_{(\mathrm{Tbase\text{-}2})}$ for TC-MI with the unadjusted CFSv2 hindcast temperature (both daily-Linvill and daily-Triangular datasets). We determined the CFSv2 hindcast skills at different lead times by using three indicators: correlation coefficient (*r),* model efficiency score (EF), and RMSE. These indicator scores were computed between the predicted bloom dates and the observation. The CFSv2 exhibits a subseasonal hindcast in bloom dates up to 6 weeks for both locations as described by *r*, EF, and RMSE in Table 2 and Fig. 6. However, the CFSv2 correlations are persistently high (above 0.75) and significant, exceeding the 99% confidence level up to the 44-day (40-day) lead time at WP-UT (TC-MI). Overall, these performance metrics suggest a poor prediction skill beyond 6 weeks.

The CFSv2 forecast skills were validated with the hindcast at 0-day lead time (which only used the observed temperature) (Fig. 2 Steps D and E). The CFSv2 shows a good performance in predicting bloom dates up to 13-days in advance at WP-UT and 10-days in advance at TC-MI (Figs. 6a, 6b), with an error of 5 days for WP-UT and 4 days for TC-MI. Beyond the 6-week lead time, the CFSv2 forecast skills in terms of *r*, EF, and RMSE are consistent with the ability for the CFSv2 to predict the winter air temperature as shown in Saha et al. (2014).

We present the time series of observed and predicted bloom dates to validate the CFSv2 predictability using daily-Linvill and daily-Triangular datasets (Fig. 7). Figures 7a1 and 7b1 confirm the high forecast skill of CFSv2 for up to a 2-week lead time for predicted bloom dates which are comparable to the observed bloom dates and predicted bloom dates by using observed temperature data. The moderate predictability is presented by Figs. 7a2-

a3 and 7b2-b3 and shows large errors in some years with EF ≥ 0.5. Large deviations between the predicted bloom dates and observations are frequently observed when lead times are beyond 6 weeks (Figs. 7a4, 7b4), suggesting poor predictability (EF < 0.5). The prediction using daily-Linvill shows slightly higher performance than those of daily-Triangular for WP-UT and vice versa for the TC-MI (Table 2). Nonetheless, the performance of using both datasets is consistent across lead times (Figs. 7a1-a4, 7b1-b4).

3.2.2 Predictability of adjusted-CFSv2 data

The CFSv2 model provides low resolution (> 50 km). Thus, we needed to adjust means and variation to be close to the observed data before incorporating into the phenological models. We tested the prediction by using only the daily-Linvill dataset and present the results in Table 2 and Fig. 6. The prediction was successfully improved by using adjusted-CFSv2 data (CFS_{adj}) up to a 40-day lead time for TC-MI as indicated by reduced RMSE and increases in EF (dotted lines, Fig. 6b). The error decreased approximately by 1 day and the EF increased to 0.90 (0.53) for the 10-day (40-day) lead time. This provides a higher confidence to predicting bloom dates compared to the unadjusted CFSv2 forecast skills. In contrast, the CFS_{adj} forecast skills for WP-UT are lower than those of the unadjusted CFSv2 throughout the 44-day lead times (dotted lines, Fig. 6a).

The results suggest that CFS_{adj} can be used for predicting bloom dates in TC-MI while the unadjusted CFSv2 is appropriate for use in WP-UT. It might be inappropriate to downscale the CFSv2 output using the aforementioned bias correction approaches for Utah because the observed and CFSv2 data did not correlate well for the entire time series. The intervening contradiction of the two datasets likely enlarges the differences in mean and variation (black-dash boxes, Fig. S2). The deviation of CFSv2 data from the observation may be caused by its low forecast skill for mountainous terrain like Utah with respect to the higher skill in a Midwest region like Michigan (e.g. Tian et al., 2017). Thus, most CFSv2 data likely show better correlations in Michigan than those Utah (Fig. S3). At each study location, deviation of the two datasets are similar for the other lead times and years (Figs. S4–S17).

4. Discussion

Even though the *Utah* model is widely used and was validated in both Utah and Michigan, we found that the prediction of bloom dates at West Payson, Utah was improved using modified Utah and original ASYMCUR models whereas adjusted T_{base} in ASYMCUR model is better suited for Traverse City, Michigan. The modification of the *Utah* model may be necessary because of the marked winter and spring warming trends in the current decade (Cayan et al. 2001; Dettinger et al. 2004; Hamlet et al. 2005; McCabe and Wolock 2007; Gillies et al. 2012). There are several studies of inaccurate use of the *Utah* model in warm climate (Pérez et al., 2008; Luedeling et al., 2011; Zhang et al., 2011) and these all showed that the model has to be modified (e.g. Positive Utah Model, Linsley-Noakes et al., 1995; North Carolina Model, Shaltout and Unrath, 1983). It appears that the extended temperature scales for chill unit contribution of 1.0 in *Utah$_{(modified)}$* model (Fig. 3) improves the estimation of chill units compared to the original *Utah* model. On the other hand, the original *Utah* model may still be suitable for use in the colder winter temperature in Michigan (with its later bloom dates than Utah).

Because of the small temperature ranges for the study sites, we analyzed temperature trends during 1980–2016 using daily temperature data from nearby stations (Provo BYU, West Payson, Utah, 40.245ºN, -111.651ºW, 1392.9 m a.s.l.; Traverse City Cherry CPTL AP, Traverse City, Michigan, 40.740ºN, -85.582ºW, 188.4 m a.s.l). The frequency of daily minimum temperature within the 1.5–12.4 ºC range (temperature scale for positive chill unit, see Fig. 3) and 2.9–9.1 ºC range (temperature scale for maximum positive chill unit—1.0, see Fig.3) decreased in September for Utah while slightly changed in Michigan (Fig. S18). Likewise, the frequency of daily maximum temperatures in those ranges decreased in December for Utah and increased in Michigan (Fig. S18). These results lend support to the use of $Utah_{(modified)}$ model in Utah by expanding the temperature range for 1.0 chill unit (see Fig. 3), otherwise the model prediction in some years could not obtain the 954 chill accumulation that is required for the rest completion of tart cherry. While both study areas undergo a warming trend in winter (Figs. S19, S22), their temperature distributions are different (Figs. S18–S24).

While the adjusted ASYMCUR model also predicts Michigan's bloom dates well, it is not clear if a 2 ºC base temperature is physiologically realistic. The phenological models are based on air temperature; nonetheless, temperature-related humidity might be the main trigger of the spring budburst of trees (Laube et al., 2014). The primary meteorological difference between study sites during the period when heat accumulation starts (February–March) were air temperature and humidity. Michigan is colder and more humid than Utah (Figs. S25–S27). Laube et al. (2014) conducted controlled-environment studies and observed that higher humidity during forcing advanced bud break in a number of deciduous tree species. From this, they hypothesized that bud rehydration is important in the forcing phase and absolute air humidity lead to phenological responses. The role of rehydration in the heat requirements is unclear. Additional field data are required for validation.

5. Conclusion

The prevailing trends of early onset and anomalously warm springs can lead to early blossoming of tart cherry and increasing risk to production from late spring freezes. In the goal of reducing risk, our study presents the first subseasonal prediction of bloom dates for Utah and Michigan. We applied a hybrid forecast approach which combines chill-forcing models with CFSv2 temperature forecasts. The *Utah* and ASYMCUR models, originally developed for fruit trees in Utah and Michigan, were modified to improve the bloom date depiction. Depicting bloom dates in Michigan were most successful with the original *Utah* and ASYMCUR$_{(Tbase-2)}$ models, whereas the *Utah*$_{(modified)}$-ASYMCUR model outperforms the original models in Utah. This difference may reflect the different winter climate in the two places.

The CFSv2 can predict bloom dates of tart cherries for 6 weeks in advance, exhibiting a reliable predictability for up to 2 weeks prior to the bloom dates with an error range within 4 days. This result suggests a potentially useful prediction to be implemented starting on 15 March for Utah and 1 April for Michigan, allowing extra time for growers to prepare and manage their orchards for possible freezes in order to reduce the risk of damage. Given the mountainous terrain in northern Utah, application of dynamical downscaling methods (e.g., application of regional climate model) may improve the predictive capabilities of CFSv2.

Acknowledgements

This research was supported by US Department of Energy grant DE-SC0016605, the Bureau of Reclamation WaterSMART program under Award Number R18AC0018, and the Utah Agricultural Experiment Station Grants Program, Utah State University (journal paper number 9107).

References

Anderson JL, Richardson EA, Kesner CD (1986) Validation of chill unit and flower bud phenology models for 'Montmorency' sour cherry. Acta Hortic. 184: 71–78.

Augspurger CK (2013) Reconstructing patterns of temperature, phenology, and frost damage over 124 years: Spring damage risk is increasing. Ecol. 94(1): 41–50. https://doi.org/10.1890/12-0200.1.

Ault TR, Henebry GM, De Beurs KM, Schwartz MD, Betancourt JL, Moore D (2013) The false spring of 2012, earliest in north America record. EOS 94(20): 181–188.

Bennett JP (1949) Temperature and bud rest period. Calif. Agric. November: 9–12.

Black B, Frisby J, Lewers K, Takeda F, Finn C (2008) Heat unit model for predicting bloom dates in Rubus. Hort. Sci. 43: 2000–2004.

Bonhomme R (2000) Bases and limits to using "degree-day" units. Eur .J. Agron. 13:1–10. https://doi.org/10.1016/S1161-0301(00)00058-7.

Cayan DR, Dettinger MD, Kammerdiener SA, Caprio JM, Peterson DH (2001) Changes in the onset of spring in the western United States. Bull. Amer. Meteor. Soc. 82(3): 399–415. https://doi.org/10.1175/1520-0477(2001)082%3C0399:CITOOS%3E2.3.CO;2.

Cesaraccio C, Spano D, Snyder RL, Duce P (2004) Chilling and forcing model to predict bud-burst of crop and forest species. Agric. For. Meteorol. 126: 1–13. https://doi.org/10.1016/j.agrformet.2004.03.002.

Chuine I, Bonhomme M, Legave JM, De Cortázar-Atauri IG, Charrier G, Lacointe A, Améglio T (2016) Can phenological models predict tree phenology accurately in the future? The unrevealed hurdle of endodormancy break. Global Change Biol. 22: 3444–3460. https://doi.org/10.1111/gcb.13383.

Cortázar-Atauri IG, Brisson N, Gaudillere JP (2009) Performance of several models for predicting budburst date of grapevine (*Vitis vinífera* L.). Int. J. Biometeorol. 53: 317–326. https://doi.org/10.1007/s00484-009-0217-4.

Dettinger MD, Cayan DR, Meyer MK, Jeton AE (2004) Simulated hydrologic responses to climate variations and change in the Merced, Carson, and American River basins, Sierra Nevada, California, 1900–2099. Clim. Change 62: 283–317. https://doi.org/10.1023/B:CLIM.0000013683.13346.4f.

Ellwood ER, Temple SA, Primack RB, Bradley NL, Davis CC (2013) Record-breaking early flowering in the eastern United States. PLoS One 8(1): e53788. https://doi.org/10.1371/journal.pone.0053788.

Erez A, Fishman S, Linsley-Noakes GC, Allan P (1990) The dynamic model for rest completion in peach buds. Acta. Hortic. 276: 165–174.

Fishman S, Erez A, Couvillon GA (1987a) The temperature- dependence of dormancy breaking in plants - computer- simulation of processes studied under controlled temperatures. J. Theor. Biol. 126(3): 309–321. https://doi.org/10.1016/S0022-

5193(87)80237-0.

Fishman S, Erez A, Couvillon GA (1987b). The temperature dependence of dormancy breaking in plants: mathematical analysis of a two-step model involving a cooperative transition. J. Theor. Biol. 124(4): 473–483. https://doi.org/10.1016/S0022-5193(87)80221-7.

Fu YH, Campioli M, Demarée G, Deckmyn A, Hamdi R, Janssens IA, Deckmyn G (2012) Bayesian calibration of the unified budburst model in six temperate tree species. Int. J. Biometeorol. 56(1): 153–64. https://doi.org/10.1007/s00484-011-0408-7.

Gillies RR, Wang S-Y, Booth MR (2012) Observational and synoptic analyses of the winter precipitation regime change over Utah. J. Clim. 25: 4679–4698. https://doi.org/10.1175/JCLI-D-11-00084.1.

Hamlet AF, Mote PW, Clark MP, Lettenmaier DP (2005) Effects of temperature and precipitation variability on snowpack trends in the Western United States. J. Clim. 18(21): 4545–4561. https://doi.org/10.1175/JCLI3538.1.

Hänninen H (1995) Effects of climatic change on trees from cool temperature regions: an ecophysiological approach to modeling of bud burst phenology. Can. J. Bot. 73(2): 183–199. https://doi.org/10.1139/b95-022.

Hawkins E, Osborne TM, Ho CK, Challinor AJ (2013) Calibration and bias correction of climate projections for crop modelling: An idealised case study over Europe. Agric. For. Meteorol. 170: 19–31. http://doi.org/http://dx.doi.org/10.1016/j.agrformet. 2012.04.007.

Linsley-Noakes GC, Louw M, Allan P (1995) Estimating daily positive Utah chill units using daily minimum and maximum temperatures. J. S. Afr. Soc. Hort. Sci. 5(1): 19–23.

Linvill DE (1990) Calculating chilling hours and chill units from daily maximum and minimum temperature observations. HortScience 25(1): 14-16.

Longstroth M (2007) Spring freezes and fruit bud damage. Michigan State University Extension. http://msue.anr.msu.edu/news/spring_freezes_and_fruit_ bud_damage. Accessed 2 Jan 2018.

Luedeling E, Brown PH (2011) A global analysis of the comparability of winter chill models for fruit and nut trees. Int. J. Biometeorol. 55: 411–421. https://doi.org/10.1007/s00484-010-0352-y.

Laube J, Sparks TH, Estrella N, Menzel A (2014) Does humidity trigger tree phenology? Proposal for an air humidity based framework for bud development in spring. New Phytol. 202, 350–355. https://doi.org/10.1111/nph.12680.

Maulión E, Valentini GH, Kovalevski L, Prunello M, Monti LL, Daorden ME, Quaglino M, Cervigni GDL (2014) Comparison of methods for estimation of chilling and heat requirements of nectarine and peach genotypes for flowering. Sci. Hortic. 177: 112–117. https://doi.org/10.1016/j.scienta.2014.07.042.

McCabe GJ, Wolock DM (2007) Warming may create substantial water supply shortages in the Colorado River basin. Geophys. Res. Lett. 34(22). https://doi.org/10.1029/2007GL031764.

Melo-Abreu JPD, Barranco D, Cordeiro AM, Tous J, Rogado BM, Villalobos FJ (2004) Modelling olive flowering date using chilling for dormancy release and thermal time.

Agric. For. Meteorol. 125(1–2): 117–127. https://doi.org/10.1016/j.agrformet.2004.02.009.

Miranda C, Santesteban, LG, Royo JB (2013) Evaluation and fitting of models for determining peach phenological stages at a regional scale. Agric. For. Meteorol. 178-179: 129-139. https://doi.org/10.1016/j.agrformet.2013.04.016.

Nash JE, Sutcliffe JV (1970) River flow forecasting through conceptual models part I — A discussion of principles. J. Hydrol. 10 (3): 282–290. https://doi.org/10.1016/0022-1694(70)90255-6

Navarro-Racines CE, Tarapues-Montenero JE (2015) Bias-correction in the CCAFS-climate portal: a description of methodologies. http://ccafs-climate.org/downloads/docs/BC_methods_explaining_v2_jrv.pdf. Accessed 15 August 2018.

NASS (the National Agricultural Statistics Service) (2002) Cherry Production. Agricultural Statistics Board, U.S. Department of Agriculture, Washington, D.C. http://usda.mannlib.cornell.edu/usda/nass/CherProd//2000s/2002/CherProd-07-01-2002.pdf. Accessed 22 January 2018.

Pérez FJ, Ormeño NJ, Reynaert B, Rubio S (2008) Use of the dynamic model for the assessment of winter chilling in a temperate and a subtropical climatic zone of Chile. Chil. J. Agric. Res. 68: 198–206. http://dx.doi.org/10.4067/S0718-58392008000200010.

Richardson EA, Seeley SD, Walker DR (1974) A model for estimating the completion of rest for ‘Redhaven’ and ‘Elberta’ peach trees. HortScience 9(4): 331–332.

Richardson EA, Anderson JL, Hatch AH, Seeley SD (1982) ASYMCUR, and asymmetric curvilinear fruit tree model. XXI Int. Hortric. Congr. 2: 2078.

Rill L (2016) Climatology of Springtime Freeze Events in the Great Lakes Region and Their Impact on Sour Cherry Yields in Historical and Projected Future Time Frames. Thesis, Michigan State University.

Saha S, Moorthi S, Wu X, Wang J, Nadiga S, Tripp P, Behringer D, Hou Y-T, Chuang H-Y, Iredeli M, Ek M, Meng J, Yang R, Mendez MP, van den Dool H, Zhang Q, Wang, W, Chen M, Becker E (2014) The NCEP Climate Forecast System Version 2. J. Clim. 27: 2185–2208. http://dx.doi.org/10.1175/JCLI-D-12-00823.1.

Schwartz MD, Ahas R, Aasa A (2006) Onset of spring starting earlier across the Northern Hemisphere. Global Change Biol. 12: 343–351. https://doi.org/10.1111/j.1365-2486.2005.01097.x.

Schwartz MD, Ault AR, Betancourt JL (2013) Spring onset variations and trends in the continental United States: past and regional assessment using temperature-based indices. Int. J. Climtol. 33: 2917–2922. https://doi.org/10.1002/joc.3625.

Shaltout AD, Unrath CR (1983) Rest completion prediction model for Starkrimson Delicious apples. J. Am. Soc. Hortic. Sci. 108(6): 957– 961.

Tian D, Wood EF, Yuan X (2017) CFSv2-based sub-seasonal precipitation and temperature forecast skill over the contiguous United States. Hydrol. Earth Syst. Sci. 21: 1477–1490. https://doi.org/10.5194/hess-1477-2017.

USDA (United States Department of Agriculture, National Agricultural Statistics Service) (2017) Statistics by State (Annual Statistical Bulletin).

https://www.nass.usda.gov/Statistics_by_State. Accessed 16 November 2017.

Warmund MR (2015) Blueberry chilling model dilemmas. J. Am. Pomol. Soc. 69(1): 26–30.

Warmund MR, Krumme J (2005) A chilling modelt o estimate rest completion of erect blackberries. HortScience 40(5): 1259–1262.

Weinberger JH (1950) Chilling requirements of peach varieties. Proc. Am. Soc. Hortic. Sci. 56: 122–128.

Zhang J, Taylor C (2011) The dynamic model provides the best description of the chill process on 'Sirora' pistachio trees in Australia. HortScience 46(3): 420–425.

Table 1 List of abbreviations used for phenological models.

Abbreviation	Description
a. Parameters	
A	Amplitude of the growth curve (TO-TB)
CH	Chill units
DL	Daylength (in hour)
F	Stress factor of fruit tree (1.0)
GDH	Growing degree hours
T	Temperature (°C)
TB	Base temperature (original TB is 4 °C; adjusted TB is 2 °C)
TH	Hourly temperature (°C)
TM	Maximum critical temperature (36 °C)
Tmax	Daily maximum temperature (°C)
Tmin	Daily minimum temperature (°C)
TO	Optimum temperature (25 °C)
Ts	Sunset temperature (°C)
b. Models	
ASYMCUR	Original Asymmetric curvilinear model (heat or forcing model) with using 4 °C as TB
$\text{ASYMCUR}_{(\text{Tbase-2})}$	Modified ASYMCUR model with using 2 °C as TB
Utah	Original Utah model (Chill model)
$\textit{Utah}_{(\text{modified})}$	Modified Utah model

Table 2 Performance of the *Utah*$_{(modified)}$-ASYMCUR and *Utah*-ASYMCUR$_{(Tbase-2)}$ to predict bloom dates for West Payson and Traverse City by using observed and unadjusted-CFS (CFS)/adjusted-CFS (CFS$_{adj}$) temperature (daily-Linvill and daily-Triangular datasets); CORR is correlation coefficient, EF is model efficiency; RMSE is root mean square error.

Location	**Dataset [Lead time]***	**CFS (Triangular)**			**CFS (Linvill)**			**CFS$_{adj}$ (Linvill)**		
		CORR	**EF**	**RMSE**	**CORR**	**EF**	**RMSE**	**CORR**	**EF**	**RMSE**
West Payson, UT	**Observation (OB) [0d]**	**0.93**	**0.57**	**5.71**	**0.94**	**0.69**	**4.82**	**0.94**	**0.69**	**4.82**
	OB+CFS0415[13d]	0.90	0.64	5.22	0.89	0.70	4.79	0.91	0.66	5.03
	OB+CFS0401[28d]	0.69	0.25	7.51	0.73	0.46	6.40	0.67	0.29	7.30
	OB+CFS0315[44d]	0.81	0.44	6.49	0.78	0.56	5.73	0.70	0.32	7.16
	OB+CFS0301[59d]	0.51	-1.42	13.5	0.49	-0.84	11.8	0.41	-0.38	10.2
	OB+CFS0215[72d]	0.40	-1.55	13.9	0.38	-0.89	11.9	0.57	-0.43	10.4
	OB+CFS0201[87d]	0.67	-0.16	9.36	0.62	0.09	8.28	0.68	-0.03	8.82
Traverse City, MI	**Observation (OB) [0d]**	**0.99**	**0.91**	**2.78**	**0.99**	**0.89**	**2.95**	**0.99**	**0.89**	**2.95**
	OB+CFS0501[11d]	0.96	0.80	4.01	0.96	0.78	4.25	0.98	0.90	2.87
	OB+CFS0415[26d]	0.85	0.41	6.94	0.87	0.38	7.11	0.85	0.55	6.07
	OB+CFS0401[41d]	0.91	0.54	6.11	0.92	0.46	6.60	0.89	0.53	6.20
	OB+CFS0315[57d]	0.75	0.09	8.61	0.74	0.00	9.01	0.73	-0.22	9.95
	OB+CFS0301[72d]	0.57	0.26	7.78	0.59	0.31	7.50	0.56	0.02	8.91
	OB+CFS0215[85d]	0.48	0.06	8.75	0.48	0.09	8.61	0.51	-0.47	10.9
	OB+CFS0201[100d]	0.54	-0.02	9.11	0.61	0.25	7.79	0.62	-0.01	9.09

* Lead time (days) before bloom dates [Lincoln Point: 28 April (averaged 2005-2016), Traverse City: 11 May (averaged 2001-2014)]

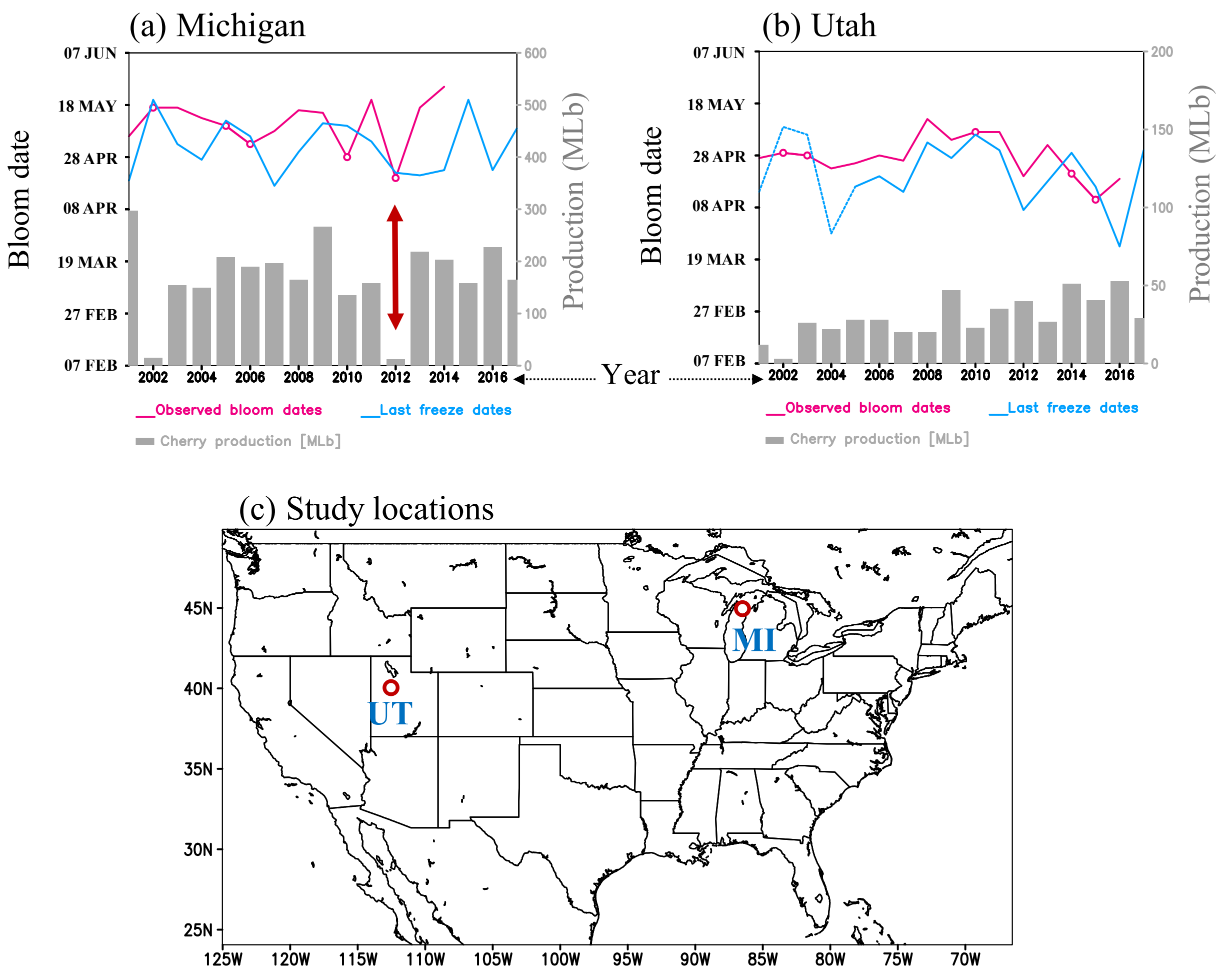

Fig. 1 Observed bloom dates, last freeze dates and state's cherry production (2001-2017) for (a) Traverse City, Michigan and (b) West Payson, Utah. (c) Study locations indicated by red circles (UT: Utah and MI: Michigan). [Cherry production data are from USDA, 2017].

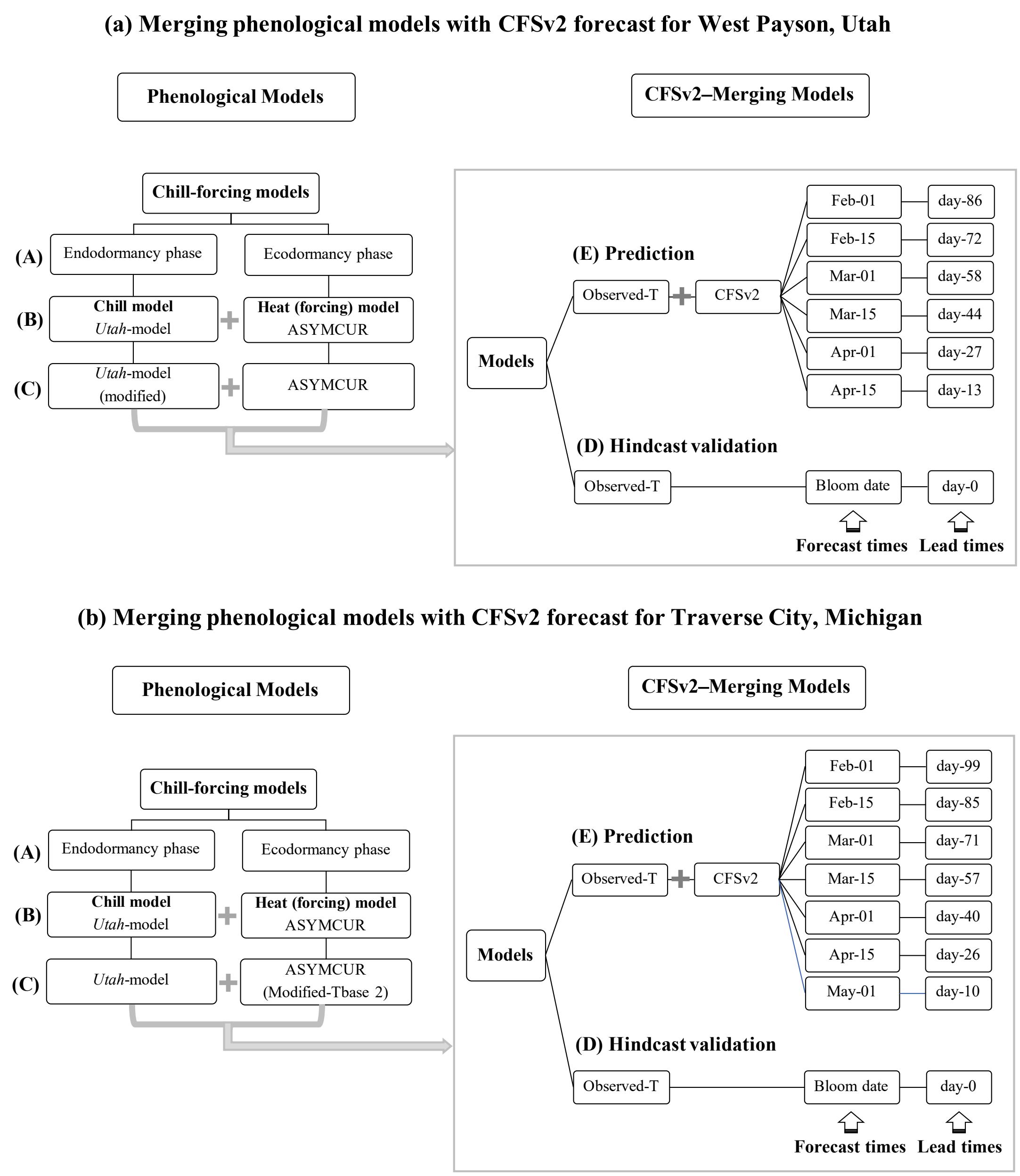

Fig. 2 Diagrams of methodological approaches to predict bloom dates by merging phenological models with CFSv2 forecast constructed for (a) West Payson, Utah and (b) Traverse City, Michigan; step (A) presents phenological phases, step (B) presents original chill-heat models, step (C) presents modified chill-heat models, step (D) presents hindcast validation using observed temperature as input, and step (E) presents bloom date prediction using observed temperature and CFSv2-forecast temperature.

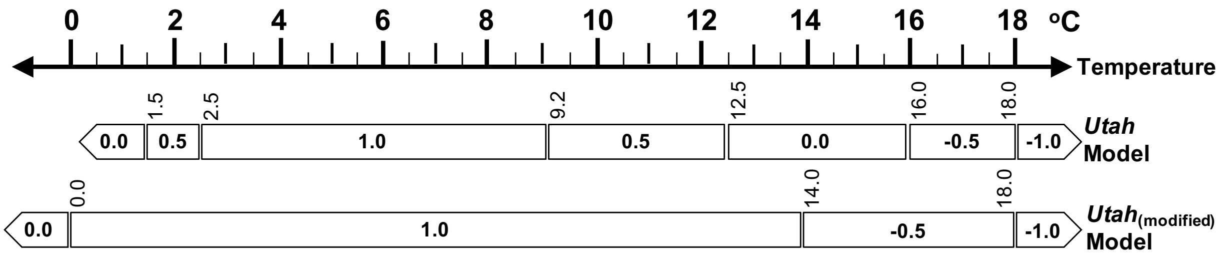

Fig. 3 Chill unit contribution (-1.0 to 1.0) from different temperature scales of *Utah* Model and Modified *Utah* Model.

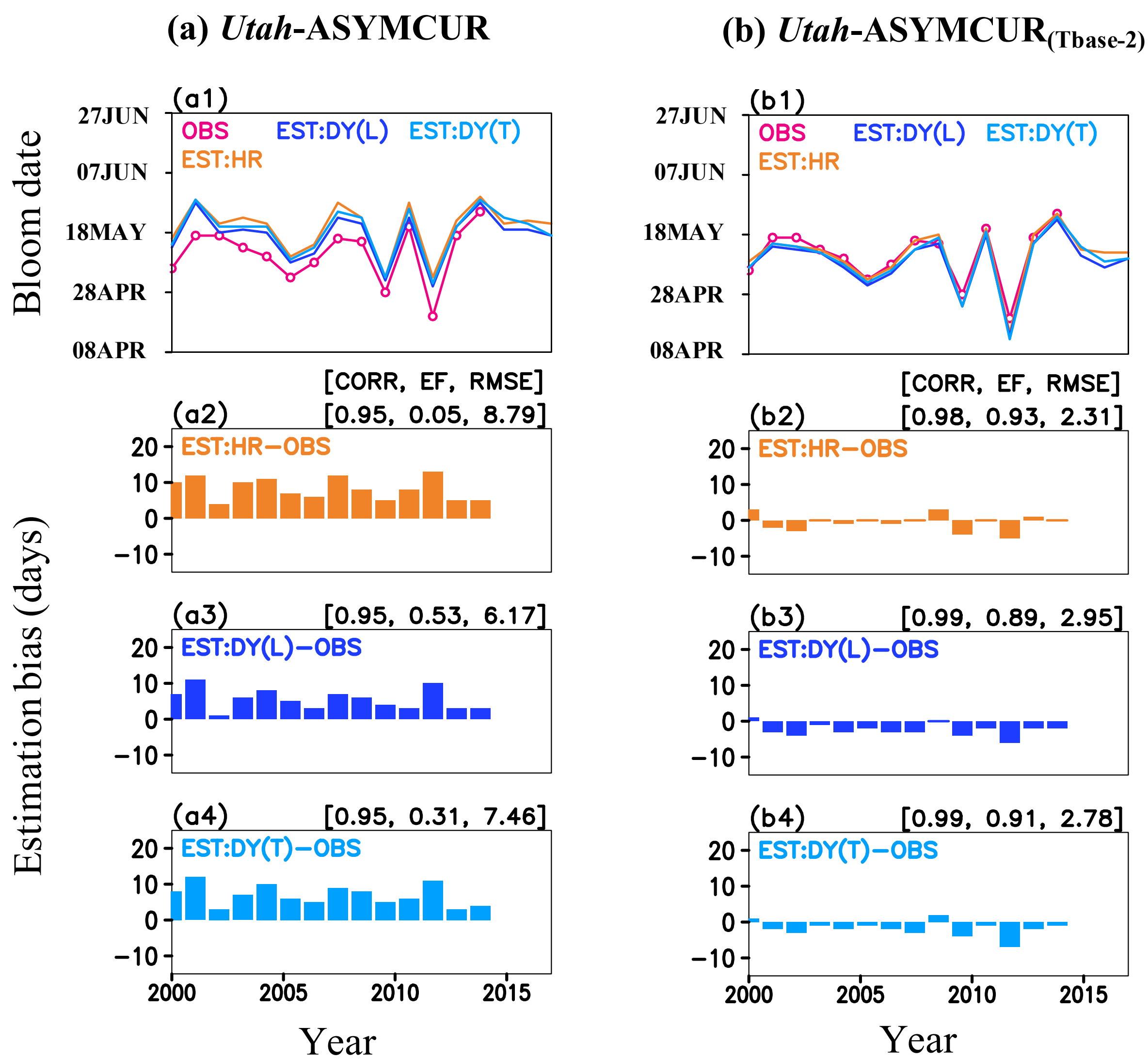

Fig. 4 (a1) Observed (OBS) and estimated (EST) bloom dates for Michigan computed by using *Utah*-ASYMCUR and three hourly-temperature datasets: observation (EST:HR) and estimation by using Linvill's method [EST:DY(L)] and Triangular method [EST:DY(T)]; (a2)-(a4) the estimation bias (EST-OBS) of EST:HR, EST:DY(L), and EST:DY(T). (b1)-(b4) are the same as (a1)-(a4) but the EST computed by using *Utah*-ASYMCUR$_{(Tbase-2)}$. Numbers in parentheses indicate correlation coefficients (CORR), model efficiency (EF), and root mean square error (RMSE), respectively.

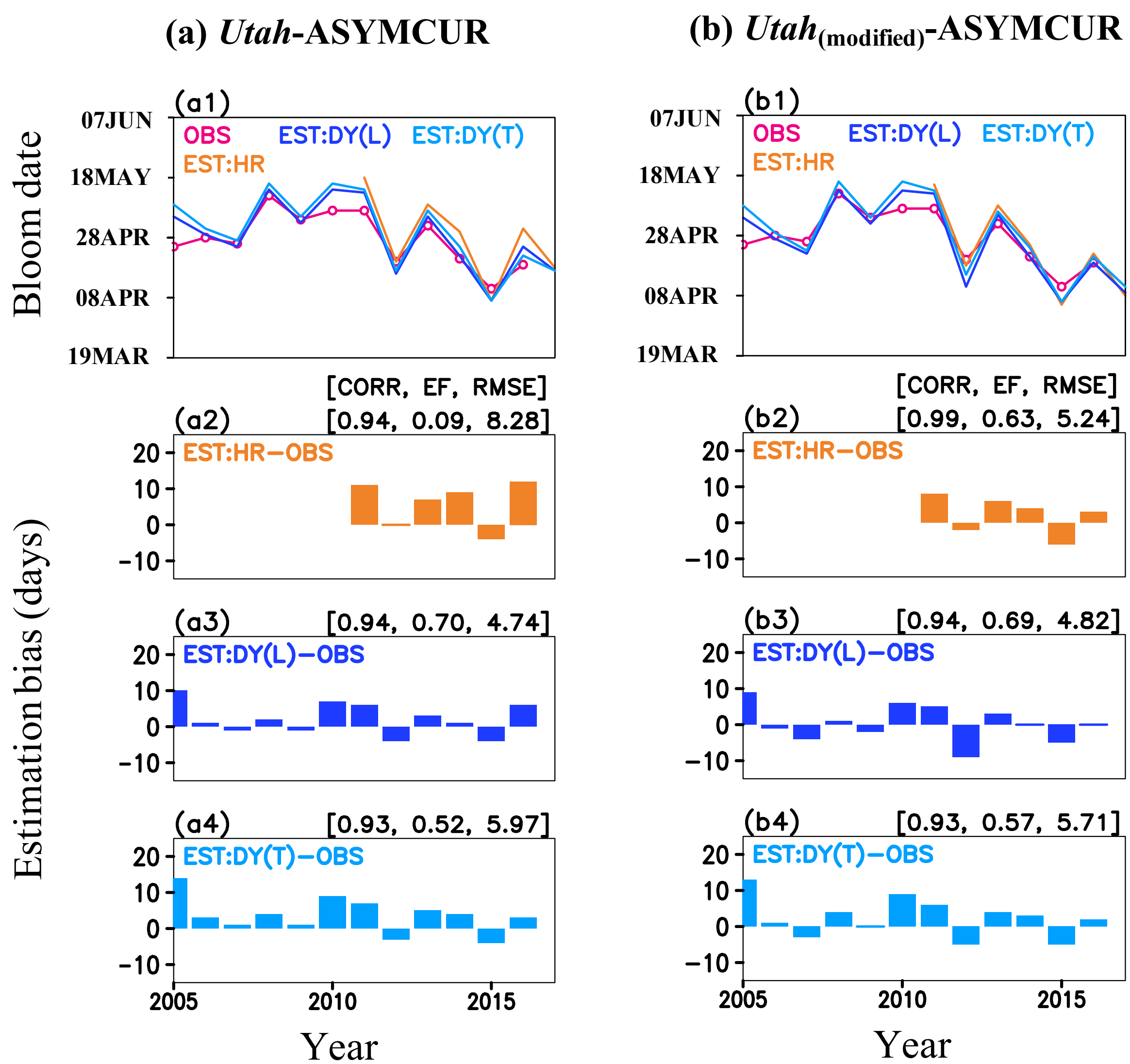

Figure 5 (a1) Observed (OBS) and estimated (EST) bloom dates for Utah computed by using *Utah*-ASYMCUR and three hourly-temperature datasets: observation (EST:HR) and estimation by using Linvill's method [EST:DY(L)] and Triangular method [EST:DY(T)]; (a2)-(a4) the estimation bias (EST-OBS) of EST:HR, EST:DY(L), and EST:DY(T). (b1)-(b4) are the same as (a1)-(a4) but the EST computed by using combined *Utah*$_{\text{(modified)}}$-ASYMCUR. Numbers in parentheses indicate correlation coefficients (CORR), model efficiency (EF), and root mean square error (RMSE), respectively.

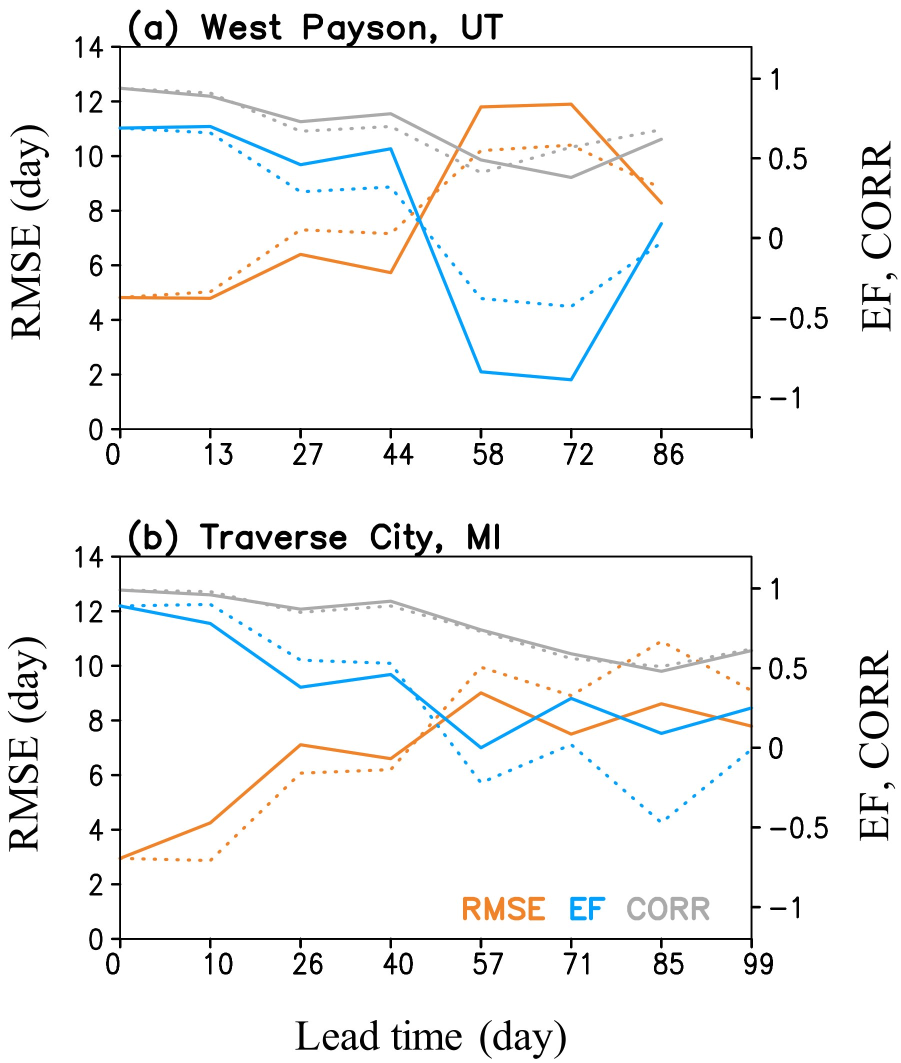

Fig. 6 Prediction performance for bloom dates indicated by correlation coefficient (CORR), model efficiency (EF), and root mean square error (RMSE) as a function of forecast time for the unadjusted-CFS (CFS; solid lines) and adjusted-CFS (CFS_{adj}; dashed lines) constructed for (a) West Payson, UT and (b) Traverse City, MI. [The hourly temperature was estimated by using Linvill's method].

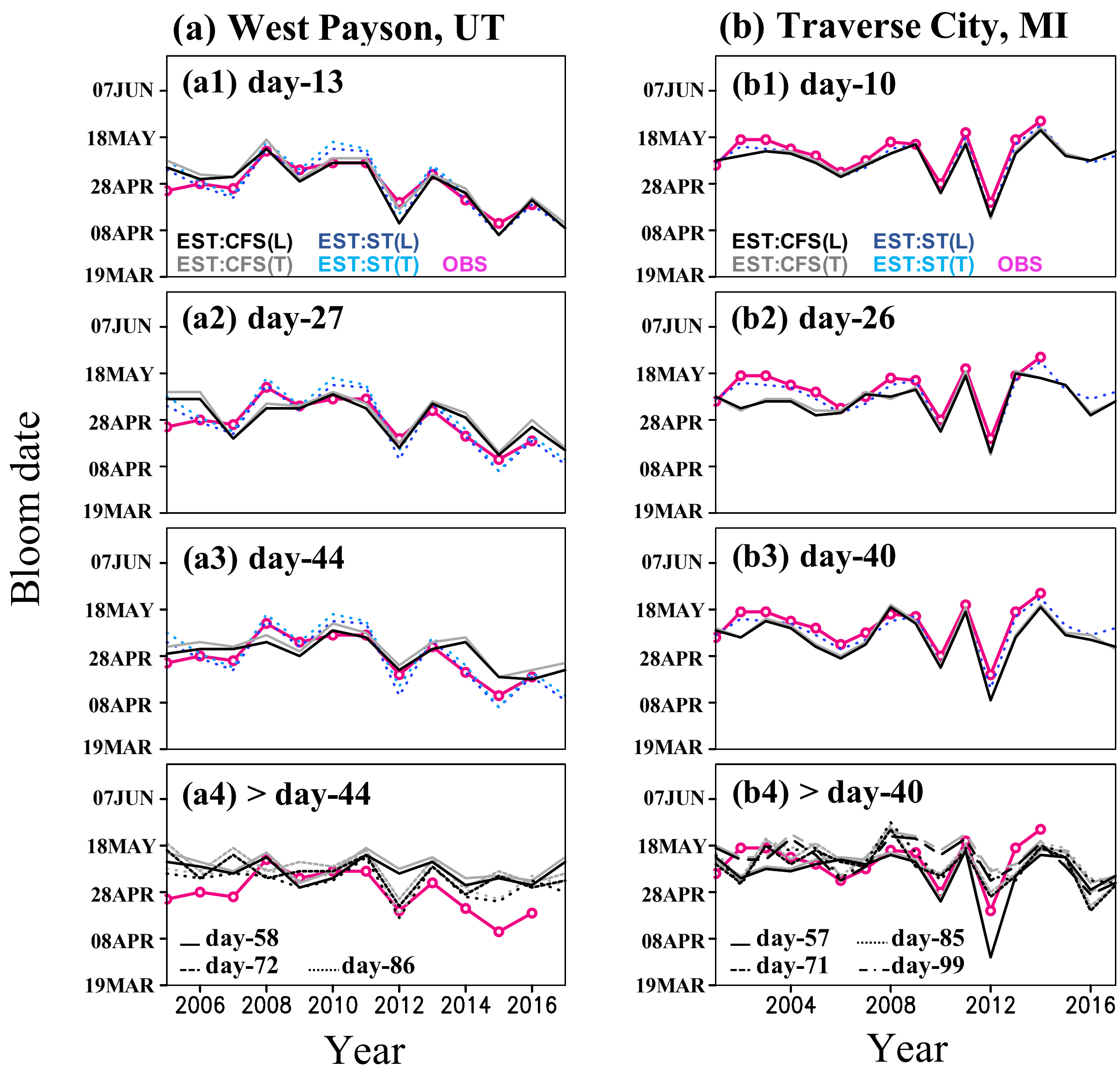

Fig. 7 Observed (OBS) and predicted (EST) bloom dates for (a) Utah and (b) Michigan computed by using estimated-hourly temperature (L: Linvill's method, T: Triangular method) from weather station and unadjusted-CFS datasets for different lead times (day); EST:ST represents 0-day lead time, EST:CFS represents lead times from 13-day (a1) or 11-day (b1) to 87-day (a4) or 100-day (b4). [Average of observed bloom date for UT is 28 April and MI is 11 May].